Molecular Biology of the Cell
Vol. 18, 3883–3893, October 2007

CDK-5 Regulates the Abundance of GLR-1 Glutamate Receptors in the Ventral Cord of *Caenorhabditis elegans*

Peter Juo,*† Tom Harbaugh,‡ Gian Garriga,‡ and Joshua M. Kaplan*

*Department of Molecular Biology, Massachusetts General Hospital, and Department of Genetics, Harvard Medical School, Boston, MA 02114; ‡Department of Molecular and Cell Biology, University of California, Berkeley, CA 94720; and †Department of Physiology, Tufts University School of Medicine, Boston, MA 02111

Submitted September 14, 2006; Revised June 21, 2007; Accepted July 20, 2007
Monitoring Editor: Francis Barr

The proline-directed kinase Cdk5 plays a role in several aspects of neuronal development. Here, we show that CDK-5 activity regulates the abundance of the glutamate receptor GLR-1 in the ventral cord of *Caenorhabditis elegans* and that it produces corresponding changes in GLR-1–dependent behaviors. Loss of CDK-5 activity results in decreased abundance of GLR-1 in the ventral cord, accompanied by accumulation of GLR-1 in neuronal cell bodies. Genetic analysis of *cdk-5* and the clathrin adaptin *unc-11* AP180 suggests that CDK-5 functions prior to endocytosis at the synapse. The scaffolding protein LIN-10/Mint-1 also regulates GLR-1 abundance in the nerve cord. CDK-5 phosphorylates LIN-10/Mint-1 in vitro and bidirectionally regulates the abundance of LIN-10/Mint-1 in the ventral cord. We propose that CDK-5 promotes the anterograde trafficking of GLR-1 and that phosphorylation of LIN-10 may play a role in this process.

INTRODUCTION

Cdk5 is a cyclin-dependent kinase whose activity is largely restricted to the nervous system. Cdk5 plays a role in many cellular processes such as neuronal cell migration, axon outgrowth, and neurodegeneration (Dhavan and Tsai, 2001). In mammals, the activity of Cdk5 requires association with either of two regulatory subunits, p35 or p39 (Dhavan and Tsai, 2001). Cdk5 or p35/p39 knockout mice die perinatally, with aberrant layering of cortical neurons, likely due to cell migration defects (Ohshima *et al*., 1996; Ko *et al*., 2001).

Recent evidence suggests that Cdk5 may also regulate synaptic transmission (Dhavan and Tsai, 2001; Bibb, 2003; Samuels and Tsai, 2003). Both Cdk5 and p35 are localized to synapses, and they are present in subcellular fractions enriched for synaptic membranes (Dhavan and Tsai, 2001; Morabito *et al*., 2004). Cdk5 has been proposed to regulate neurotransmitter release by phosphorylating Munc18 and P/Q-type voltage-dependent calcium channels (Fletcher *et al*., 1999; Tomizawa *et al*., 2002) and to regulate synaptic vesicle endocytosis by phosphorylating dynamin, type I phosphatidylinositol (4) phosphate 5-kinase, amphiphysin, and synaptojanin (Samuels and Tsai, 2003; Lee *et al*., 2004, 2005).

Cdk5 has also been proposed to regulate glutamate receptor function. Fast excitatory synaptic transmission is mediated primarily by two families of glutamate receptors (GluRs): α-amino-3-hydroxy-5-methyl-4-isoxazolepropionic acid (AMPA) receptors and *N*-methyl-D-aspartate (NMDA) receptors. Work from several laboratories suggests that regulation of the abundance of postsynaptic AMPA receptors is a cellular mechanism for producing activity-dependent changes in synaptic strength, e.g., long-term potentiation (LTP), long-term depression, and homeostatic plasticity (Malinow and Malenka, 2002; Song and Huganir, 2002; McGee and Bredt, 2003; Park *et al*., 2004). Cdk5 phosphorylates PSD95 and the NMDA receptor subunit NR2A, the latter resulting in increased NMDA receptor currents (Li *et al*., 2001; Wang *et al*., 2003; Morabito *et al*., 2004). Cdk5 may also regulate synaptic plasticity, because manipulation of Cdk5 activity produces defects in LTP and spatial learning (Fischer *et al*., 2002, 2005; Ohshima *et al*., 2005).

We have used the nematode *Caenorhabditis elegans* as a genetic model to study regulation of GluR abundance at synapses. The *C. elegans* genome encodes two NMDA and eight non-NMDA receptor subunits (Brockie *et al*., 2001a), one of which is encoded by the *glr-1* gene (Hart *et al*., 1995; Maricq *et al*., 1995). The *glr-1* GluR is expressed in ventral cord interneurons (Hart *et al*., 1995; Maricq *et al*., 1995), where it is localized at sensory–interneuron and interneuron–interneuron synapses (Rongo *et al*., 1998; Burbea *et al*., 2002). We previously showed that the synaptic abundance of GLR-1 receptors is regulated by clathrin-mediated endocytosis and ubiquitin ligases (Burbea *et al*., 2002; Juo and Kaplan, 2004; Dreier *et al*., 2005), as are mammalian AMPA receptors (Carroll *et al*., 1999; Luscher *et al*., 1999; Man *et al*., 2000; Colledge *et al*., 2003; Patrick *et al*., 2003).

Here, we show that CDK-5 regulates the abundance of GLR-1 in the ventral cord, which may be mediated, in part, by the ability of CDK-5 to regulate the scaffolding protein LIN-10/Mint-1.

MATERIALS AND METHODS

Strains and Reagents

The following strains were used in this study: *nuIs24* (P*glr-1*::GLR-1::GFP), *nuIs125* (P*glr-1*::SNB-1::GFP), *nuIs1*(*Pglr-1::gfp*), *pzIs2* (*Pglr-1::cdk-5*), *nuEx993* (P*glr-1*::LIN-10::GFP), *p35(gm335), p35(tm648), cdk-5(gm336), cdk-5(ok626), unc-11(e47), glr-1 (n2461), lin-10(n1853), and lin-10(e1439).* Note that *p35* is also known as *cdka-1*. All wild-type GLR-1::GFP refers to *nuIs24* unless otherwise noted.

The *cdk-5* allele *gm336* was isolated by screening a *C. elegans* deletion library. The *gm336* mutation corresponds to a 760-base pair deletion defined

This article was published online ahead of print in *MBC in Press* (http://www.molbiolcell.org/cgi/doi/10.1091/mbc.E06–09–0818) on August 1, 2007.

Address correspondence to: Peter Juo (peter.juo@tufts.edu).

by the following endpoints (left breakpoint: tagagatttgagagacacaaacaa/right breakpoint: tacttcaattgatatgtggtctgccggg, positionally ambiguous nucleotides are underlined). The *cdk-5* allele *ok626* was isolated by the *C. elegans* Knockout Consortium and consists of a 1.6-kb deletion. Both *gm336* and *ok626* are predicted to be null alleles, because both delete the *cdk-5* start codon. The *ok626* allele also deletes part of a neighboring gene T27E9.4.

The *p35* allele *gm335* was isolated by screening a *C. elegans* deletion library. *gm335* deletes the entire coding region of *p35*. The molecular endpoints of the deletion are undefined. The *p35* deletion allele *tm648* was isolated by Shohei Mitani (National Bioresource Project) and consists of an 833-base pair deletion. The *tm648* deletion removes exons 2 and 3, and it is not likely to encode a functional protein.

Fluorescence Microscopy and Quantitation

All imaging was done using a Zeiss Axiovert 100 microscope (Carl Zeiss, Thornwood, NY) and an ORCA 100 charge-coupled device camera (Hamamatsu, Bridgewater, NJ). Larval stage 4 (L4) animals raised at 20°C were immobilized with 30 mg/ml 2,3-butanedione monoxamine (Sigma-Aldrich, St. Louis, MO) for 5 min before imaging. All images were captured and processed using MetaMorph 4.5 software (Molecular Devices, Downingtown, PA).

Quantitative analysis of puncta fluorescence was achieved using a Planapo 100× (numerical aperture = 1.4) objective (Olympus America, Melville, NY). Maximum intensity projections of Z-series stacks were obtained. Identical fluorescence filters were used for all experiments. Exposure settings and camera gain were set to fill the 12-bit dynamic range without saturation. Line scans of ventral cord puncta fluorescence were obtained using MetaMorph, and they were analyzed in Igor Pro (Wavemetrics, Lake Oswego, OR) using custom-written software (J. Dittman, Massachusetts General Hospital, Boston, MA).

Each line scan corresponded to ~60–70 μm of the ventral nerve cord. Unless otherwise noted, all images were taken from an anterior region of the ventral nerve cord just posterior to the RIG neuronal cell bodies. We also imaged a region of the ventral nerve cord just posterior to the vulva (puncta intensity [normalized] ± SEM: wild type: 1.0 ± 0.06 (n = 25), *cdk-5(gm336)*: 0.71 ± 0.07 (n = 22), $p < 0.01$; width [μm] ± SEM: wild type: 0.91±0.05, *cdk-5(gm336)*: 0.9 ± 0.08; density [puncta/10 μm] ± SEM: wild type: 1.88±0.1, *cdk-5(gm336)*: 1.76 ± 0.1). These results are similar to those observed in the anterior region of the ventral nerve cord (VNC) (Figure 2). These regions are distinct from that which was analyzed in our previous article, which was anterior to the RIG cell bodies (Juo and Kaplan, 2004); consequently, the data reported here cannot be directly compared with those reported previously. Puncta intensities, widths, and densities from each line scan were analyzed in an automated manner using Igor Pro, as described previously (Burbea *et al*., 2002). Puncta intensity was measured as the fractional increase in peak fluorescence of each punctum over the diffuse fluorescence in the ventral nerve cord (%ΔF/F). Puncta widths were determined by measuring the width of each punctum at half the maximum peak fluorescence. Puncta density was determined by the average number of puncta per 10 μm of ventral nerve cord, as described previously (Burbea *et al*., 2002). All the values reported in the figures are means ± SEM. Statistical significance was determined using the Student's *t* test.

To quantify soluble green fluorescent protein (GFP) from the *glr-1* transcriptional reporter *nuIs1*, we used MetaMorph version 7.1 software (Molecular Devices) to image the ventral nerve cords of wild-type *(nuIs1)* and *nuIs1;cdk-5(gm336)* animals. A defined region posterior to the RIG cell bodies was imaged, and the amount of soluble GFP fluorescence was quantitated using Region Statistics in MetaMorph. The values reported in the text refer to the average pixel intensities ± SEM.

To quantitate the amount of GLR-1::GFP in interneuron cell bodies, we imaged the cell body of the interneuron PVC in L4 animals and quantitated the average pixel intensities of three patches per cell body using MetaMorph version 7.1 software.

Real-Time Polymerase Chain Reaction (PCR)

Total RNA was isolated from wild-type *(nuIs24)* and *cdk-5* null mutant [*nuIs24;cdk-5(ok626)*] animals by using an RNeasy fibrous tissue kit (QIAGEN, Valencia, CA). cDNA was synthesized using Superscript II (Invitrogen, Carlsbad, CA), and real-time PCR was performed using SYBR Green and SureStart Taq (Stratagene, La Jolla, CA) and a Stratagene MxPro real-time PCR machine. Standard curves were used to calculate the relative amount of *glr-1* or *lin-10* mRNA in each sample, and they were normalized to actin mRNA.

Transgenes and Germline Transformation

Standard techniques were used to isolate transgenic strains by microinjection of various plasmids (50 ng/μl) with P*ttx3*::dsRed2 (J. Dittman) as a coinjection marker. *nuIs24*, *nuIs125*, and *nuEx993* have been described previously (Rongo *et al*., 1998; Juo and Kaplan, 2004). The *p35* (T23F11.3) and *cdk-5* open reading frames (ORFs) were obtained by reverse transcription-PCR from wild-type cDNA and subsequently subcloned under the control of the *glr-1* promoter (pV6) [pV6::p35 (KP#1413), pV6::cdk-5 (KP#1414)]. Site-directed mutagenesis was performed on pV6::cdk-5 using QuikChange mutagenesis kit (Stratagene) to mutate Asp144 to Asn in pV6::cdk-5(D144N) (KP#1415), and Lys33 to Thr in pV6::cdk-5(K33T) (KP#1416). The *lin-10* ORF was subcloned under the control of the *glr-1* promoter to create pV6::lin-10 (KP#199) as described previously (Rongo *et al*., 1998). A Not I site was introduced at the C terminus of LIN-10 just before the stop codon. The LIN-10::GFP construct was created by inserting GFP into the NotI site. Phosphomutant LIN-10(10Pm)::GFP was created by using a combination of site-directed mutagenesis and PCR-overlap extension mutagenesis. The following sites in LIN-10 were mutated to alanine in LIN-10(10Pm): S15A, T26A, T28A, S87A, S155A, S201A, T330A, T396A, T416A, S420A. GFP was introduced at the C terminus of LIN-10 by using a NotI site to create pV6::LIN-10(10Pm)::GFP. All constructs were confirmed by sequencing. Full details of plasmids and oligonucleotides are available upon request.

Behavior Assays

Nose touch assays were preformed as described previously (Kaplan and Horvitz, 1993). Briefly, young adult wild-type, *cdk-5(gm336)*, *cdk-5(ok626)*, or *glr-1(n2461)* animals were placed on a thin lawn of OP50 *Escherichia coli* and assayed for nose touch responses to an eyelash. Each animal was scored 10 times. For locomotion assays, young adult wild-type animals, overexpressing *Pglr-1::cdk-5(pzIs2)*, *glr-1(n2461)*, and *Pglr-1::cdk-5(pzIs2);glr-1(n2461)* double mutant animals were transferred with halocarbon oil (Sigma-Aldrich) to an NGM plate without food. After 2 min of equilibration, the number of reversals/min was recorded for a total of 5 min/animal. Both behavioral assays were performed by an experimenter unaware of the mutant genotypes (i.e., in a blind manner).

Kinase Assays

Full-length LIN-10, LIN-10(ΔC) (amino acids [aa] 1–572), and LIN-10(ΔN) (aa 565-954) were N-terminally tagged with glutathione *S*-transferase (GST), expressed in bacteria and purified using standard techniques. GST-tagged substrates were incubated in a 30-μl reaction with [γ^{32}P]ATP and kinase buffer (50 mM HEPES, pH 7, 10 mM $MgCl_2$, 100 μm ATP, 1 mM dithiothreitol, 50 mM β-glycerolphosphate) for 30 min at 37°C either with or without purified, recombinant CDK5/p25 (a gift from L.-H. Tsai, MIT, MA). Kinase assay reactions were stopped with 30 μl of 2X sample buffer (250 mM Tris, pH 6.8, 4% SDS, 10% β-mercaptoethanol, 15% glycerol, and 0.25% bromophenol blue), and analyzed on SDS-polyacrylamide gels, stained with Coomassie Brilliant Blue, dried and autoradiographed.

RESULTS

CDK-5 and p35 Regulate the Abundance of GLR-1 in the Ventral Nerve Cord

We visualized GLR-1 containing synapses by examining the distribution of a GFP-tagged GLR-1 (GLR-1::GFP) in the ventral nerve cord (VNC). Expression of GLR-1::GFP in the ventral cord interneurons rescues the mechanosensory behavioral defects of *glr-1* null mutant animals, indicating that GLR-1::GFP is functional (Rongo *et al*., 1998). GLR-1::GFP has a punctate pattern of localization in the VNC interneurons (Rongo *et al*., 1998). Greater than 80% of the GLR-1::GFP puncta are closely apposed by the presynaptic markers synaptobrevin and the vesicular glutamate transporter (VGLUT), indicating that GLR-1::GFP localizes to postsynaptic elements (Burbea *et al*., 2002).

To test whether CDK-5 regulates GLR-1 trafficking, we analyzed the distribution of GLR-1::GFP in two *p35* deletion mutants, *p35(tm648)* and *p35(gm335)* (*p35* is also known as *cdka-1*; see *Materials and Methods*), using quantitative fluorescence microscopy. To estimate the amount of GLR-1::GFP in each punctum, we measured the fluorescence intensities (%ΔF/F) and widths of each punctum, as described previously (see *Materials and Methods*) (Burbea *et al*., 2002). To assess changes in the number of GLR-1-containing synapses in the ventral cord, we measured the density of GLR-1::GFP puncta. GLR-1::GFP puncta intensities were significantly decreased in both *p35* mutants (Figure 1, A–C and E), whereas puncta densities were unchanged (data not shown). The decreased puncta intensities observed in *p35(gm335)* mutants were corrected by expression of wild-type *p35* cDNA in ventral cord interneurons, by using the *glr-1* promoter

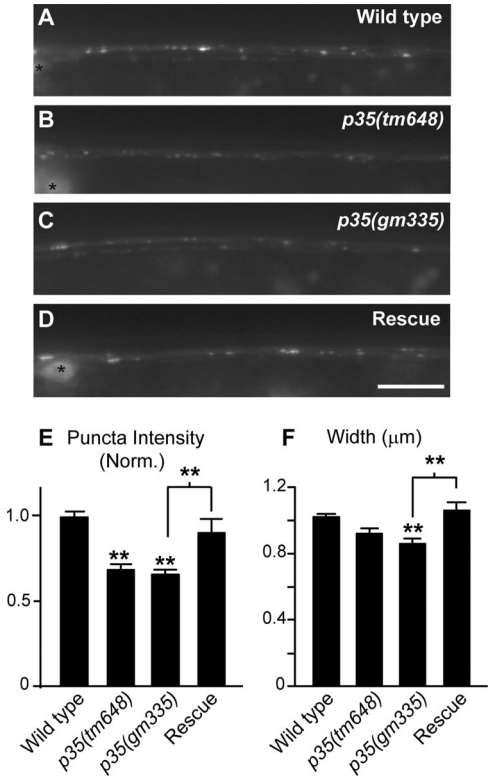

Figure 1. p35 functions in the ventral cord to regulate the abundance of GLR-1::GFP. GLR-1::GFP puncta in the anterior ventral nerve cord of L4 wild-type (A), *p35(tm648)* (B), *p35(gm335)* (C), and rescued *p35(gm335)* (D) animals were imaged. The decreased GLR-1::GFP puncta intensities in *p35* loss-of-function mutants was rescued by introduction of wild-type *p35* cDNA under the control of the *glr-1* promoter (D). Puncta intensities (normalized) (E) and widths (F) were compared in wild-type (n = 121), *p35(tm648)* (n = 21), *p35(gm336)* (n = 40), and rescued *p35(gm336)* (n = 22) animals. For each image, anterior is to the left and ventral is up; asterisks indicate cell bodies of GLR-1–expressing cells. Error bars represent SEM. Bar, 10 μm. Values that differ significantly (Student's *t* test) from wild-type controls are marked by asterisks above each bar, whereas other comparisons are marked by brackets. Significant differences are indicated as follows: $p < 0.01$ (*) or $p < 0.001$ (**).

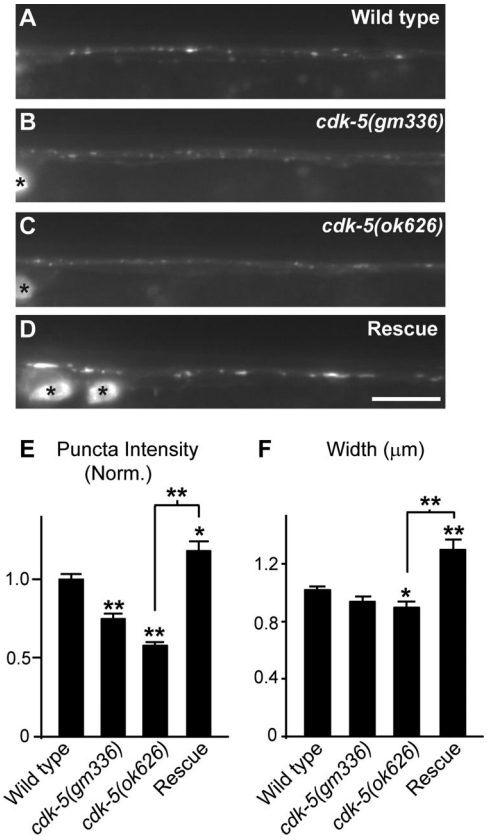

Figure 2. CDK-5 functions in the ventral cord to regulate the abundance of GLR-1::GFP. GLR-1::GFP puncta in the anterior ventral nerve cord of L4 wild-type (A), *cdk-5(gm336)* (B), and *cdk-5(ok626)* (C) animals were imaged. The decreased GLR-1::GFP puncta intensities in *cdk-5* loss-of-function mutants was corrected by introduction of wild-type *cdk-5* cDNA under the control of the *glr-1* promoter (D). Puncta intensities (normalized) (E) and widths (F) were compared in wild-type (n = 121), *cdk-5(gm336)* (n = 56), *cdk-5(ok626)* (n = 51), and rescued *cdk-5(ok626)* (n = 24) animals. For each image, anterior is to the left and ventral is up; asterisks indicate cell bodies of GLR-1–expressing cells. Error bars represent SEM. Bar, 10 μm. Values that differ significantly (Student's *t* test) from wild-type controls are marked by asterisks above each bar, whereas other comparisons are marked by brackets. Significant differences are indicated as follows: $p < 0.01$ (*) or $p < 0.001$ (**).

(Figure 1, D–F) (Hart *et al*., 1995; Maricq *et al*., 1995). These data indicate that *p35* functions in interneurons to regulate GLR-1::GFP abundance in the ventral cord.

We also analyzed the distribution of GLR-1::GFP in the ventral cords of two *cdk-5* deletion mutants *cdk-5(gm336)* and *cdk-5(ok626)*. Both *cdk-5* alleles are predicted to be molecular nulls (see *Materials and Methods*). GLR-1::GFP puncta intensities decreased in both *cdk-5(gm336)* and *cdk-5(ok626)* mutants compared with wild-type controls (Figure 2, A–C and E). GLR-1::GFP puncta densities were modestly reduced (13%; $p < 0.001$) in *cdk-5(ok626)*, but they were unchanged in *cdk-5(gm336)* (data not shown). The decreased puncta intensities in *cdk-5(ok626)* were corrected by expression of wild-type *cdk-5* cDNA in the interneurons (Figure 2, D and E). Expression of wild type *cdk-5* cDNA in *cdk-5(ok626)* also increased GLR-1::GFP puncta widths compared with wild-type controls (Figure 2, A, D, and F), most likely due to overexpression of CDK-5. These data indicate that *cdk-5* functions in the interneurons to regulate GLR-1::GFP abundance in the ventral cord, and the magnitude of this effect was similar to that observed in *p35* mutants (Figure 1).

To test whether the kinase activity of CDK-5 is required for regulation of GLR-1, we analyzed the distribution of GLR-1::GFP in strains containing transgenes driving expression of kinase-inactive *cdk-5* in interneurons. Overexpression of *cdk-5* in wild-type animals increased the intensities and widths of GLR-1::GFP puncta (Figure 3, A and B, G and H), whereas transgenes driving expression of two catalytically inactive CDK-5 mutants (K33T and D144N) (Nikolic *et al*., 1996) did not increase puncta fluorescence (Figure 3, A–D, G, and H). The failure of these mutant constructs to increase GLR-1 abundance in the cord could be caused by decreased stability of the mutant proteins; however, equivalent point mutations in mammalian Cdk5 did not affect protein stability in cultured cells (Nikolic *et al*., 1996). Overexpressing CDK-5(D144N) produced a slight decrease ($p < 0.01$) in GLR-1::GFP puncta fluorescence (Figure 3G), suggesting that this mutant protein must be expressed at sufficiently high levels to produce dominant-negative activity. The increased GLR-1::GFP abundance caused by overexpression of CDK-5 was eliminated in mutants lacking *p35* (Figure 3, A,

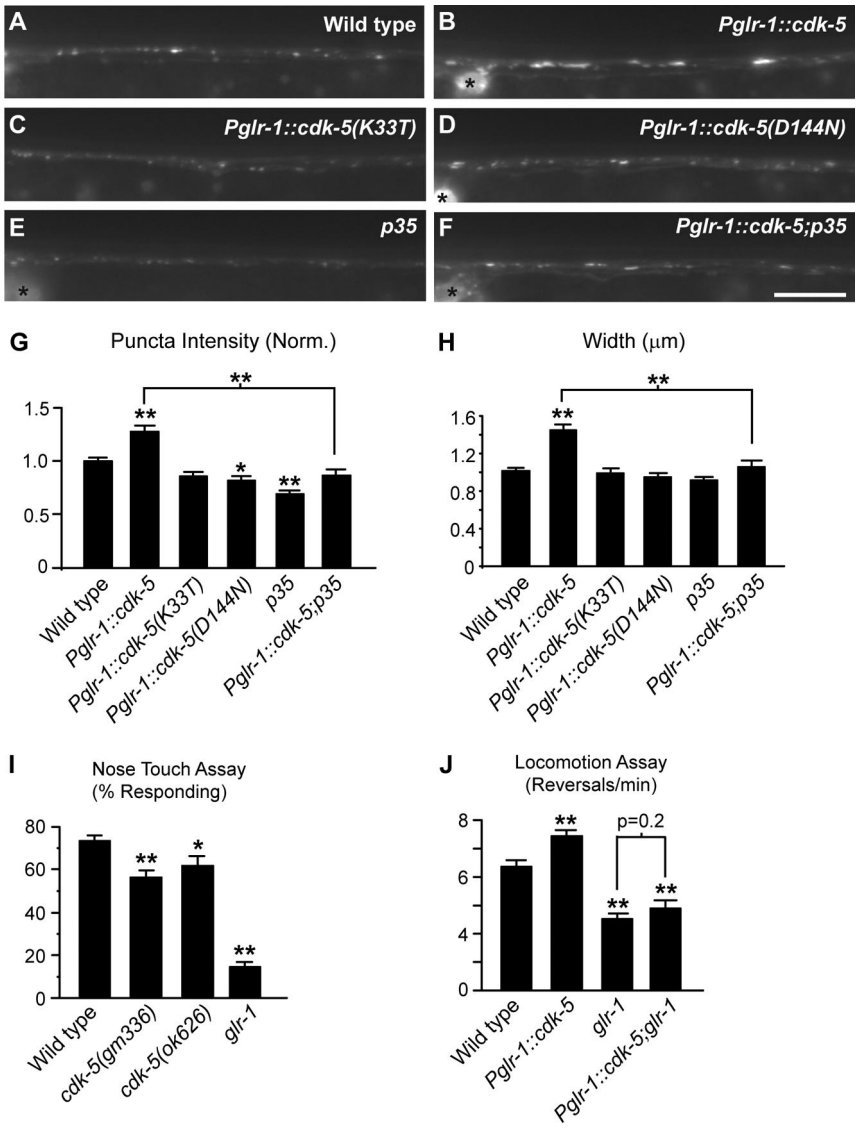

Figure 3. CDK-5 regulation of GLR-1::GFP requires the kinase domain and the regulatory subunit, p35, and it alters GLR-1–mediated behaviors. Expression of wild-type *cdk-5* cDNA under the *glr-1* promoter increases the abundance of GLR-1::GFP in the ventral cord. GLR-1::GFP puncta in the anterior ventral nerve cord of L4 wild-type animals (A); animals expressing wild-type *cdk-5* cDNA (B); animals expressing two different versions of kinase-dead *cdk-5*, *Pglr-1::cdk-5(K33T)* (C) and *Pglr-1::cdk-5(D144N)* (D); *p35(tm648)* mutants (E); and animals expressing wild-type *cdk-5* in *p35(tm648)* mutants, *Pglr-1::cdk-5;p35* (F), were imaged. Puncta intensities (normalized) (G) and widths (H) were compared in wild-type (n = 121), *Pglr-1::cdk-5* (n = 63), *Pglr-1::cdk-5(K33T)* (n = 25), *Pglr-1::cdk-5(D144N)* (n = 24), *p35(tm648)* (n = 21), and *Pglr-1::cdk-5;p35(tm648)* (n = 23) animals. (I) Responses to nose touch were determined for wild-type (n = 52), *cdk-5(gm336)* (n = 53), *cdk-5(ok626)* (n = 32), and *glr-1(n2461)* (n = 50) animals. (J) Reversal frequencies were assayed for wild-type (n = 41), *Pglr-1::cdk-5* (n = 37), *glr-1(n2461)* (n = 36), and *Pglr-1::cdk-5;glr-1(n2461)* (n = 20) animals. For each image, anterior is to the left and ventral is up; asterisks indicate cell bodies of GLR-1–expressing cells. Error bars represent SEM. Bar, 10 μm. Values that differ significantly (Student's *t* test) from wild-type controls are marked by asterisks above each bar, whereas other comparisons are marked by brackets. Significant differences are indicated as follows: $p < 0.01$ (*) or $p < 0.001$ (**).

B, and E–H), suggesting that endogenous p35 is required for this effect. These results indicate that CDK-5/p35 catalytic activity bidirectionally regulates GLR-1::GFP levels in the ventral cord.

The decreased abundance of GLR-1::GFP in *cdk-5* null mutants could be due to decreased *glr-1* transcription. We tested this possibility by analyzing expression of a *glr-1* transcriptional reporter, *nuIs1 (Pglr-1::gfp)* and by measuring the levels of *glr-1* mRNA by using real-time PCR. We found that the levels of soluble GFP in the ventral nerve cord of wild-type and *cdk-5* null mutants were not significantly different (average intensity values ± SEM: wild type: 1769 ± 52 AU, n = 22; *cdk-5(gm336)*: 1725 ± 56 arbitrary units [AU], n = 21). Similarly, the abundance of *glr-1* mRNA was not significantly different between wild-type and *cdk-5* null mutant animals (mean *glr-1* mRNA levels ± SEM normalized to actin mRNA: wild-type animals = 0.82 ± 0.1, n = 4; *cdk-5(ok626)* null mutant animals = 1.08 ± 0.2, n = 6; Student's *t* test, p = 0.2). These results indicate that the decreased GLR-1::GFP abundance in the ventral nerve cord of *cdk-5* null mutants was not caused by decreased *glr-1* transcription.

CDK-5 Regulates GLR-1–dependent Behaviors

If CDK-5 regulates the abundance of GLR-1 at synapses, we might expect an effect on GLR-1 function and a consequent change in behavior. Two simple behavioral assays can be used to assess the function of GLR-1–containing synapses: the nose touch assay and locomotion (Hart *et al*., 1995; Maricq *et al*., 1995; Zheng *et al*., 1999). Gentle touch to the nose of the worm results in a mechanosensory reflex that induces backward locomotion. Mutants with defects in glutamatergic signaling, such as *glr-1* or *eat-4* VGLUT (a presynaptic vesicular glutamate pump) nulls are less responsive to nose touch (Hart *et al*., 1995, 1999; Maricq *et al*., 1995; Berger *et al*., 1998). We found that *cdk-5* null mutant animals had decreased responses to nose touch compared with wild-type controls (Figure 3I; Student's *t* test, $p < 0.01$ for both *cdk-5* alleles). We also tested whether increased CDK-5 activity affected locomotion behavior. *C. elegans* moves in a sinusoidal pattern and alternates between periods of forward and reverse locomotion. The frequency of reversals is dependent on the amount of glutamatergic signaling. For example, mutants with decreased glutamatergic signaling,

such as *glr-1* or *eat-4* VGLUT mutants, have decreased reversal frequencies compared with controls (Zheng *et al*., 1999; Brockie *et al*., 2001b; Burbea *et al*., 2002; Juo and Kaplan, 2004; Schaefer and Rongo, 2006) (Figure 3J). Conversely, mutants with increased glutamatergic signaling have increased reversal frequencies compared with controls (Zheng *et al*., 1999; Burbea *et al*., 2002; Juo and Kaplan, 2004; Schaefer and Rongo, 2006). We found that animals overexpressing *cdk-5* under the *glr-1* promoter *(Pglr-1*::*cdk-5)* had increased reversal frequencies compared with wild-type controls (Figure 3J), as would be predicted if glutamatergic signaling were increased. Furthermore, the increased reversal frequency caused by overexpressed *cdk-5 (Pglr-1*::*cdk-5)* was suppressed in *glr-1* null mutant animals (Figure 3J), suggesting that CDK-5 regulation of locomotion behavior is dependent on endogenous GLR-1. Thus, CDK-5 activity bidirectionally regulates GLR-1::GFP abundance in the ventral cord, and produces corresponding changes in GLR-1–mediated behaviors.

The Distribution of Synaptobrevin Was Not Altered in cdk-5 Mutants

To determine whether CDK-5 regulates the trafficking of other synaptic proteins, we examined the distribution of the synaptic vesicle protein, synaptobrevin, tagged with GFP (SNB-1::GFP). The intensities, widths, and densities of SNB-1::GFP puncta were unaltered in both *cdk-5(gm336)* and *cdk-5(ok626)* compared with wild-type controls (Figure 4, A–C). These results suggest that the effects of CDK-5 on GLR-1::GFP are unlikely to be a secondary consequence of decreased synaptic inputs, because the density of presynaptic SNB-1::GFP puncta was normal in *cdk-5* mutants. Cdk5 has been implicated in synaptic vesicle endocytosis; however, we did not observe increased, diffuse SNB-1::GFP fluorescence in the ventral cord, which is characteristically found in other endocytic mutants (Jorgensen *et al*., 1995; Burbea *et al*., 2002; Schuske *et al*., 2003; Dittman and Kaplan, 2006). These results do not exclude the possibility that CDK-5 regulates synaptic vesicle endocytosis, as has been suggested previously (Samuels and Tsai, 2003; Lee *et al*., 2004; Lee *et al*., 2005), because our analysis is likely insensitive to small changes in endocytosis (Dittman and Kaplan, 2006). Together, our results are most consistent with the idea that CDK-5 directly regulates some aspect of GLR-1 trafficking.

CDK-5 Acts Early in the Secretory Pathway to Regulate GLR-1

Cdk5 has been implicated in regulating both anterograde trafficking (Ratner *et al*., 1998; Dhavan and Tsai, 2001; Morfini *et al*., 2004), and endocytic recycling of cargo proteins (Samuels and Tsai, 2003; Lee *et al*., 2004, 2005). Either of these functions could explain the effects of CDK-5 on the distribution of GLR-1::GFP. The decreased GLR-1::GFP observed in *cdk-5* mutants could result from increased postendocytic degradation of GLR-1 or from decreased anterograde trafficking of GLR-1 to the VNC. To distinguish between these possibilities, we analyzed *unc-11; cdk-5* double mutants (Figure 5, A–F). Null mutations in *unc-11*, which encodes the clathrin adaptin AP180, have defects in clathrin-mediated endocytosis (Zhang *et al*., 1998; Nonet *et al*., 1999), resulting in the accumulation of GLR-1::GFP in the VNC (Figure 5, A and B) (Burbea *et al*., 2002). If GLR-1::GFP endocytosis is enhanced in a *cdk-5* loss-of-function mutant, then the distribution of GLR-1::GFP in *unc-11;cdk-5* double mutants should be similar to that seen in *unc-11* single mutants, because *unc-11* AP180 mutations should block this enhanced retrieval. By contrast, we found that *unc-11;cdk-5* double mutants had

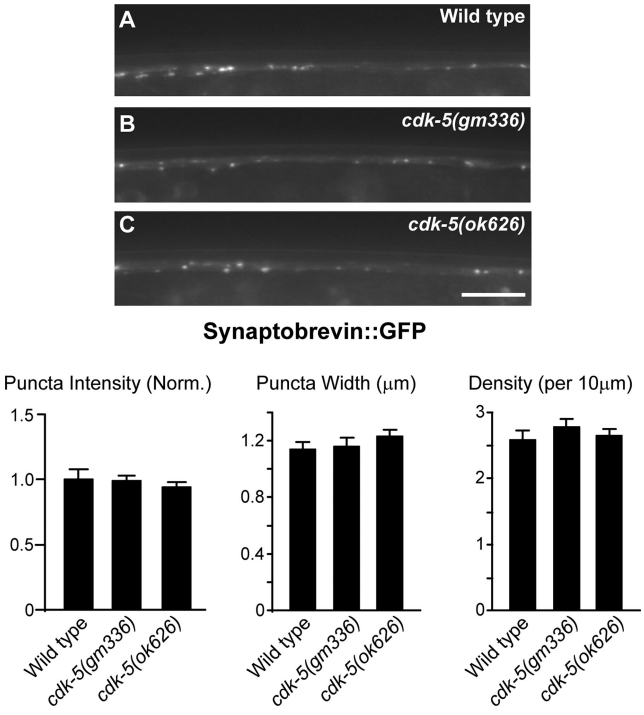

Figure 4. *cdk-5* mutants do not affect the distribution of GFP-tagged synaptobrevin. Synaptobrevin::GFP puncta in the anterior ventral nerve cord of L4 wild-type (A), *cdk-5(gm336)* (B), and *cdk-5(ok626)* (C), animals were imaged. Puncta intensities (normalized), widths, and densities were compared in wild-type (n = 18), *cdk-5(gm336)* (n = 19), and *cdk-5(ok626)* (n = 25) animals. For each image, anterior is to the left and ventral is up. Error bars represent SEM. Bar, 10 μm. Values that differ significantly (Student's *t* test) from wild-type controls are indicated as follows: $p < 0.01$ (*) or $p < 0.001$ (**).

GLR-1::GFP puncta intensities that were indistinguishable from those found in *cdk-5(gm336)* single mutants ($p = 0.4$) (Figure 5, C–F). Similar results were observed in *unc-11* double mutants by using the *cdk-5(ok626)* allele (data not shown). These results suggest that CDK-5 regulates a process that occurs earlier in the secretory pathway than receptor recycling, and they are consistent with a role for CDK-5 in regulating anterograde trafficking of GLR-1::GFP.

If CDK-5 regulates GLR-1 trafficking early in the secretory pathway, we would expect GLR-1 to accumulate in interneuron cell bodies of *cdk-5* null mutant animals. We tested this possibility by measuring the abundance of GLR-1::GFP in PVC interneuron cell bodies of wild-type and *cdk-5* null mutant animals. We found that GLR-1::GFP cell body fluorescence increased in two independent *cdk-5* null mutants, *cdk-5(gm336)* and *cdk-5(ok626)*, compared with wild-type controls (Figure 5, G and H). This effect was rescued by expressing wild-type *cdk-5* cDNA in the interneurons by using the *glr-1* promoter (Figure 5, G and H). This cell body accumulation is unlikely to represent a postendocytic compartment, because our double mutant analysis indicates that the CDK-5 effect was not altered by mutations that disrupt clathrin-mediated endocytosis (i.e., *unc-11* AP180). Thus, decreased GLR-1::GFP in the ventral cord is accompanied by increased abundance in cell bodies, consistent with our model that CDK-5 regulates GLR-1 trafficking early in the secretory pathway, perhaps by regulating receptor assembly or transit through the endoplasmic reticulum (ER)/Golgi.

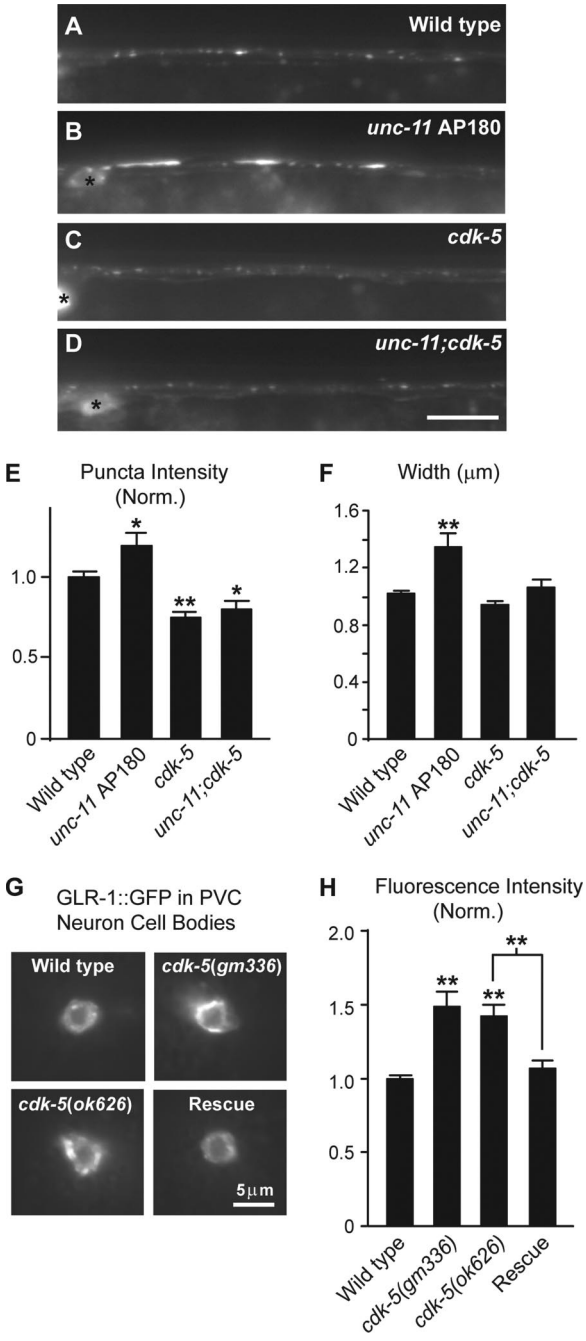

Figure 5. CDK-5 functions upstream of endocytosis. GLR-1::GFP puncta in the anterior ventral nerve cords of L4 wild-type (A), *unc-11(e55)* AP180 (B), *cdk-5(gm336)* (C), and double mutant *unc-11(e55)* AP180;*cdk-5(gm336)* (D) animals were imaged. Puncta intensities (normalized) (E) and widths (F) were compared in wild-type (n = 121), *unc-11(e47)* AP180 (n = 26), *cdk-5(gm336)* (n = 56), and double mutant *unc-11(e47)* AP180;*cdk-5(gm336)* (n = 20) animals. (G and H) GLR-1::GFP fluorescence in the cell bodies of the interneuron PVC of L4 wild-type (n = 46), *cdk-5(gm336)* (n = 20), *cdk-5(ok626)* (n = 17), and rescued *cdk-5(ok626)* (n = 30) animals were imaged (G) and quantitated (H). For each image (A–D), anterior is to the left and ventral is up; asterisks indicate cell bodies of GLR-1–expressing cells. Error bars represent SEM. Bar, 10 μm. Values that differ significantly (Student's *t* test) from wild-type controls are marked by asterisks above each bar, whereas other comparisons are marked by brackets. Significant differences are indicated as follows: $p < 0.01$ (*) or $p < 0.001$ (**).

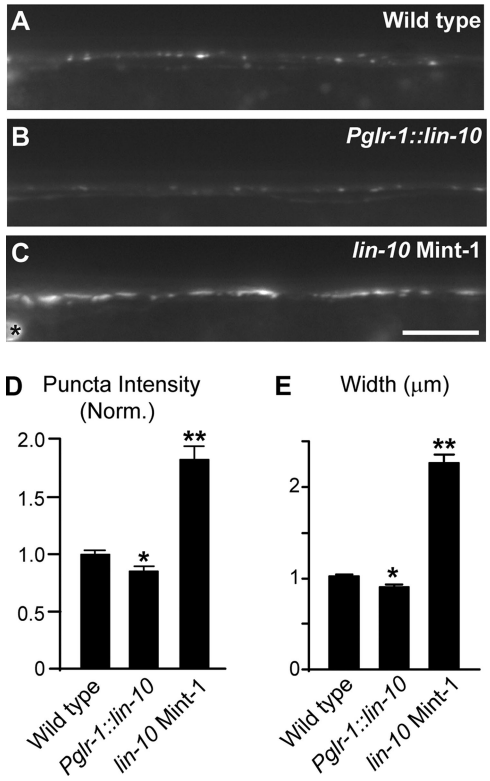

Figure 6. LIN-10/Mint-1 negatively regulates GLR-1 abundance in the ventral cord. GLR-1::GFP puncta in the anterior ventral nerve cords of L4 wild-type animals (A), animals expressing *lin-10* cDNA under the *glr-1* promoter, *Pglr-1::lin-10* (B), and *lin-10(n1853)* Mint-1 loss-of-function mutants (C), were imaged. Puncta intensities (normalized) (D) and widths (E) were compared in wild-type (n = 121), *Pglr-1::lin-10* (n = 31), and *lin-10(n1853)* Mint-1 (n = 25) animals. For each image, anterior is to the left and ventral is up; asterisks indicate cell bodies of GLR-1–expressing cells. Error bars represent SEM. Bar, 10 μm. Values that differ significantly (Student's *t* test) from wild-type controls are indicated as follows: $p < 0.01$ (*) or $p < 0.001$ (**).

CDK-5 Negatively Regulates the Abundance of LIN-10/Mint-1

What is the target of CDK-5 that mediates its effects on GLR-1::GFP? Several studies suggest that the PDZ protein LIN-10/Mint-1 may regulate anterograde membrane trafficking from the ER/Golgi to the synapse. LIN-10/Mint-1 localizes to the Golgi and to synapses, and it regulates the surface expression of AMPA receptors in mammalian hippocampal neurons (Butz *et al*., 1998; Borg *et al*., 1999; Whitfield *et al*., 1999; Tomita *et al*., 2001; Stricker and Huganir, 2003). In addition, mammalian LIN-10/Mint-1 has been proposed to act as a cargo adaptor promoting association of the kinesin KIF17 with NMDA receptor-containing transport vesicles (Setou *et al*., 2000). We showed previously that the distribution of GLR-1::GFP is abnormal in *lin-10* mutants (Rongo *et al*., 1998). The intensities and widths of GLR-1::GFP puncta increase in *lin-10(n1853)* loss-of-function mutants compared with wild-type controls (Figure 6A and C–E) (Rongo *et al*., 1998). Similar results were seen in a second loss-of-function mutant *lin-10(e1439)* (data not shown) (Rongo *et al*., 1998). Conversely, overexpression of *lin-10* cDNA in interneurons (using the *glr-1* promoter) resulted in a small but significant decrease in GLR-1::GFP puncta intensities and widths compared with wild-type controls (Figure 6, A and B, and D and E). These results indicate

that LIN-10/Mint-1 negatively regulates the abundance of GLR-1::GFP in the VNC. These findings are consistent with data from cultured rat neurons where overexpression of wild-type Mint-1 decreased GluR1 surface clusters, whereas expression of a mutant Mint-1 protein, in which the first PDZ domain was mutated, increased GluR1 clusters (Stricker and Huganir, 2003).

One potential model that could explain CDK-5 regulation of GLR-1 is that CDK-5 regulates LIN-10/Mint-1 levels. We tested this idea by examining the effects of CDK-5 activity on the abundance of LIN-10::GFP in the VNC. We previously showed that LIN-10::GFP is expressed in a punctate pattern in the ventral cord and that a subset of these puncta colocalize with GLR-1 (Rongo *et al*., 1998; Juo and Kaplan, 2004; Dreier *et al*., 2005). Overexpression of the *cdk-5* cDNA in interneurons, by using the *glr-1* promoter, decreased the intensities and density of LIN-10::GFP puncta, with no effect on puncta widths (Figure 7, A and B, E–G). Conversely, LIN-10::GFP puncta intensities increased in both *cdk-5(gm336)* and *cdk-5(ok626)* loss-of-function mutants (Figure 7, A–E). These results indicate that CDK-5 decreases the abundance of LIN-10::GFP in the ventral nerve cord. Changes in LIN-10::GFP abundance were not caused by changes in expression of the transgene because expression of the *glr-1* promoter (which was used to drive expression of this construct) was not altered in *cdk-5* mutants (detailed above). Moreover, the abundance of endogenous *lin-10* mRNA was not significantly different between wild-type and *cdk-5* null mutant animals (mean *lin-10* mRNA levels ± SEM normalized to actin mRNA: wild-type animals = 1.1 ± 0.1, n = 4; *cdk-5(ok626)* null mutant animals = 1.2 ± 0.1, n = 6; Student's *t* test, p = 0.06). These results indicate that CDK-5 regulates LIN-10::GFP abundance by a posttranscriptional mechanism.

We next tested whether CDK-5 could directly phosphorylate LIN-10. The amino-terminal half of LIN-10/Mint-1 contains 10 potential CDK-5 phosphorylation sites, Ser/Pro (SP) or Thr/Pro (TP) sequences. The amino-terminal regions of LIN-10/Mint1 proteins are not well conserved in mouse, flies, and worms; however, SP/TP sequences are found in the amino-terminal domains of all LIN-10/Mint1 orthologues, and phophoproteomic analysis indicates that LIN-10/Mint proteins are phosphorylated on SP/TP sites in mouse brain extracts (Ballif *et al*., 2004). To determine whether LIN-10/Mint-1 is a direct substrate for CDK-5, we performed an in vitro kinase assay by using recombinant mammalian Cdk5/p25 and GST-tagged LIN-10 proteins (Figure 8, A and B). p25 is a truncated, more active form of p35 (Dhavan and Tsai, 2001). Cdk5/p25 phosphorylated full-length LIN-10 and a deletion mutant lacking the C terminus (ΔC), but not a mutant lacking the N terminus (ΔN) (Figure 8B; data not shown). These results indicate that Cdk5 can directly phosphorylate the amino-terminal domain of LIN-10 in vitro.

To test the in vivo relevance of the CDK-5 phosphorylation sites, we expressed a GFP-tagged mutant protein in which all 10 SP/TP sites were mutated to alanine residues [LIN-10(10Pm)]. The intensity and density of wild-type LIN-10::GFP in the ventral nerve cord were both significantly decreased by overexpression of CDK-5 (Figure 7). By contrast, *cdk-5* overexpression did not significantly reduce the intensity (p = 0.14) or density (p = 0.28) of LIN-10(10Pm)::GFP (Figure 8, C–F). An increase in LIN-10(10Pm)::GFP puncta intensity still occurred in *cdk-5* null mutants, although the magnitude of the increase was reduced compared with wild-type LIN-10::GFP (Figure 7 and data not shown). These results suggest that phosphorylation of LIN-10 contributes to CDK-5–mediated regulation of LIN-10 abundance in vivo.

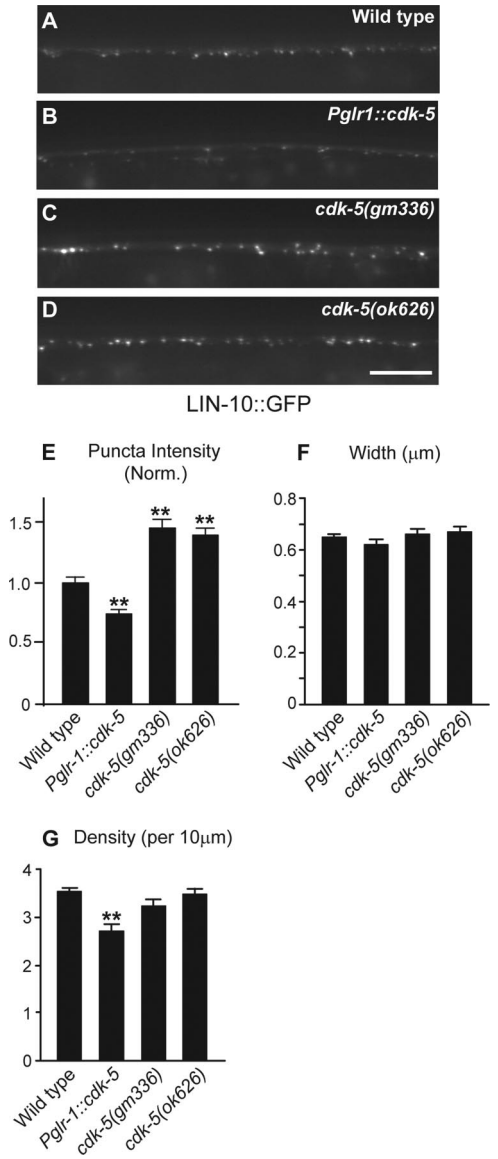

Figure 7. CDK-5 negatively regulates LIN-10/Mint-1 abundance in the ventral nerve cord. LIN-10::GFP puncta in the anterior ventral nerve cords of L4 wild-type animals (A); animals expressing *cdk-5* cDNA under the *glr-1* promoter, *Pglr-1::cdk-5* (B) and *cdk-5(gm336)* (C); and *cdk-5(ok626)* (D) animals were imaged. Puncta intensities (normalized) (E), widths (F), and densities (G) were compared in wild-type (n = 80), *Pglr-1::cdk-5* (n = 29), *cdk-5(gm336)* (n = 34), and *cdk-5(ok626)* (n = 38) animals. For each image, anterior is to the left and ventral is up. Error bars represent SEM. Bar, is 10 μm. Values that differ significantly (Student's *t* test) from wild-type controls are indicated as follows: $p < 0.01$ (*) or $p < 0.001$ (**).

Thus far, our results suggest that CDK-5 regulates LIN-10 abundance, which may contribute to CDK-5–mediated regulation of GLR-1 abundance and behaviors. To further test this idea, we analyzed GLR-1 abundance in *lin-10;cdk-5* double mutants (Figure 9). If LIN-10 is the only CDK-5 target required for regulation of GLR-1, then we would expect that CDK-5 would not be able to regulate GLR-1 in the absence of LIN-10 in a *lin-10* mutant. Instead, we found that GLR-1::GFP puncta intensities in *cdk-5;lin-10* double mutants

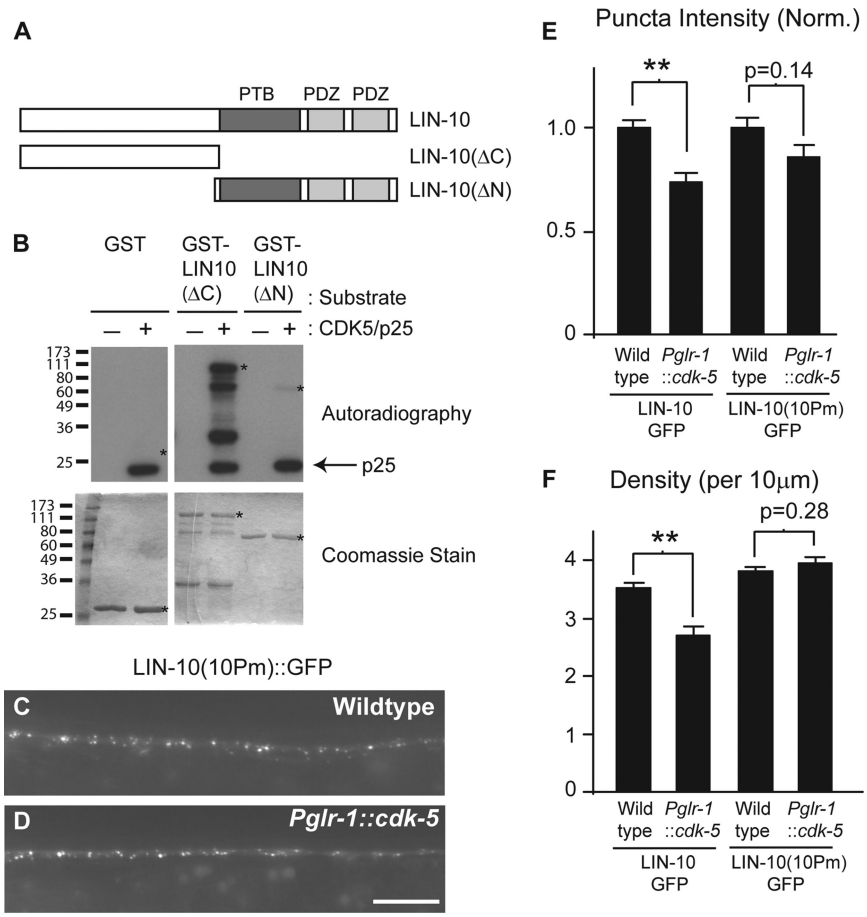

Figure 8. CDK-5 phosphorylates LIN-10/Mint-1 in vitro and phosphomutant LIN-10 blocks the effects of CDK-5 in vivo. (A) Schematic showing N-terminally GST-tagged LIN-10(ΔC) and LIN-10(ΔN). (B) Recombinant substrates GST (lanes 1 and 2), GST-LIN-10(ΔC) (lanes 3 and 4), and GST-LIN-10(ΔN) (lanes 5 and 6) were incubated with [^{32}P]ATP either without (lanes 1, 3, and 5) or with recombinant CDK-5/P25 (lanes 2, 4, and 6). The ^{32}P incorporation into substrate was monitored with autoradiography (B; top), and substrate protein levels were monitored using Coomassie stain (B; bottom). The asterisks mark the position of full-length substrates on the Coomassie-stained gel (B; bottom) and on the autoradiograph (B; top). Molecular weight is shown on the left (kilodaltons). (C and D) Phosphomutant LIN-10(10Pm)::GFP puncta in the anterior ventral nerve cord of wild-type (C) or animals expressing *cdk-5* cDNA under the *glr-1* promoter, *Pglr-1::cdk-5* (D), were imaged. Puncta intensities (E) and densities (F) were compared for wild-type LIN-10::GFP in wild type (n = 80) and *Pglr-1::cdk-5* (n = 29)–expressing animals, and for phosphomutant LIN-10(10Pm)::GFP in wild-type (n = 40) and *Pglr-1::cdk-5* (n = 26) animals. In E and F, data for wild-type LIN-10::GFP (from Figure 7) have been included for comparison. For each image, anterior is to the left and ventral is up. Error bars represent SEM. Bar, 10 μm. Values that differ significantly (Student's *t* test) from wild-type controls are marked by asterisks above each bar, whereas other comparisons are marked by brackets. Significant differences are indicated as follows: $p < 0.01$ (*) or $p < 0.001$ (**).

were intermediate in value between *cdk-5* and *lin-10* single mutants (Figure 9). These results suggest that CDK-5 must have other relevant targets, in addition to LIN-10, because CDK-5 was still able to regulate GLR-1 in *lin-10* mutants (i.e., double mutant puncta intensities were significantly lower than those found in *lin-10* single mutants).

DISCUSSION

Cdk5 participates in diverse cellular processes such as cell migration, axon outgrowth, and neurodegeneration (Dhavan and Tsai, 2001). Our results suggest that CDK-5 positively regulates the abundance of GLR-1 in the ventral cord and that it has corresponding effects on GLR-1-mediated behaviors (nose touch and locomotion). CDK-5 regulation of GLR-1 depends on its kinase activity and on the regulatory subunit *p35*. The effects of CDK-5/p35 on GLR-1 are cell autonomous and consistent with the idea that CDK-5 plays a role in regulating GLR-1 trafficking.

CDK-5 Regulation of the Polarized Protein Trafficking Machinery

The scaffolding protein LIN-10/Mint-1 is required for polarized sorting of the LET-23 epidermal growth factor receptor to the basolateral domain of epithelial cells in *C. elegans* (Kaech *et al*., 1998). In both mammals and worms, LIN-10/Mint-1 proteins have been shown to exist in heteromultimeric protein complexes containing LIN-2/CASK, LIN-7/Veli, Caskin, and SAP97 proteins (Butz *et al*., 1998; Borg *et al*., 1999). These protein complexes have been proposed to play a general role in polarized receptor trafficking in both epithelial cells and neurons (to basolateral and dendritic domains, respectively).

We showed that LIN-10/Mint-1 is likely a physiological substrate of CDK-5. Recombinant CDK-5 phosphorylated LIN-10/Mint-1 in vitro. In vivo, CDK-5 activity decreased the abundance of the scaffolding protein LIN-10/Mint-1 in the ventral cord, and a nonphosphorylatable mutant LIN-10 protein was resistant to this effect (Figures 7 and 8). These results suggest that CDK-5 is likely to directly regulate the function of protein complexes containing LIN-10/Mint-1, and thus it could potentially regulate the polarized trafficking of axonal and dendritic proteins.

What Aspect of GLR-1 Trafficking Is Regulated by CDK-5?

CDK-5/p35 seems to regulate an early step in the secretory pathway. Our data show that *cdk-5* loss-of-function mutants have decreased GLR-1::GFP in the ventral cord, whereas overexpression of *cdk-5* results in increased GLR-1::GFP (Figures 2 and 3). Loss of CDK-5 activity prevents accumulation of GLR-1::GFP in the ventral cord after blockade of clathrin-mediated endocytosis (Figure 5). This result suggests that CDK-5 regulates an aspect of GLR-1 trafficking that occurs before receptor recycling. In support of this model, GLR-1::GFP accumulates in neuronal cell bodies in *cdk-5* null mutant animals (Figure 5). Thus, CDK-5 could regulate assembly of receptors in the endoplasmic reticulum, budding of receptors from the Golgi, or anterograde transport of receptors from the Golgi to the ventral cord.

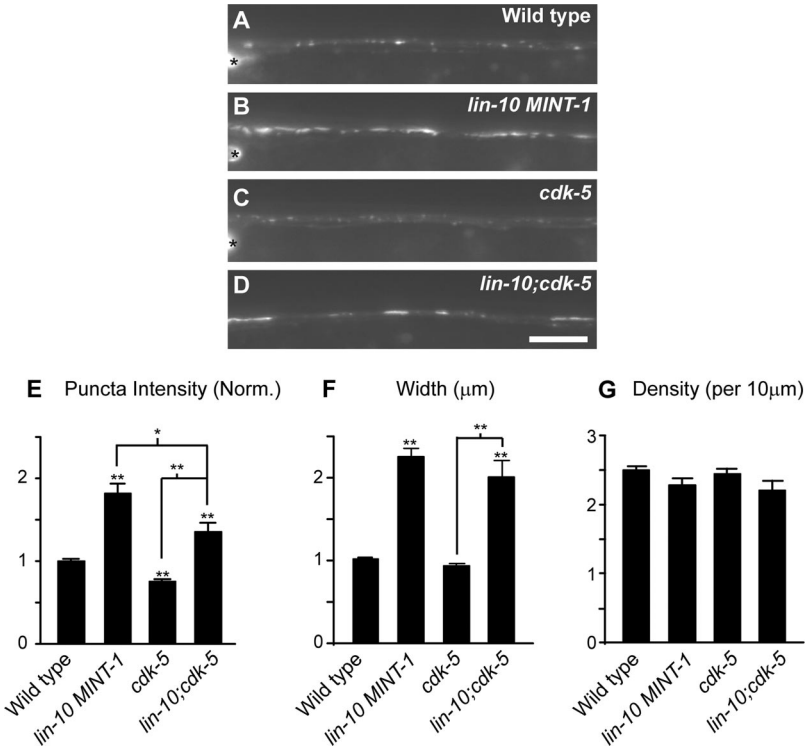

Figure 9. LIN-10 is not the only downstream mediator of CDK-5. GLR-1::GFP puncta in the anterior ventral nerve cords of L4 wild-type (A), *lin-10(n1853)* Mint-1 (B), *cdk-5(gm336)* (C), and *lin-10(n1853);cdk-5(gm336)* (D) animals were imaged. Puncta intensities (normalized) (E), widths (F), and densities (G) were compared in wild-type (n = 121), *lin-10(n1853)* Mint-1 (n = 25), *cdk-5(gm336)* (n = 56), and *lin-10(n1853);cdk-5(gm336)* (n = 25) animals. For each image, anterior is to the left and ventral is up; asterisks indicate cell bodies of GLR-1–expressing cells. Error bars represent SEM. Bar, 10 μm. Values that differ significantly (Student's *t* test) from wild-type controls are marked by asterisks above each bar, whereas other comparisons are marked by brackets. Significant differences are indicated as follows: $p < 0.01$ (*) or $p < 0.001$ (**).

Consistent with the idea that CDK-5 regulates anterograde transport of GLR-1, previous studies have suggested that Cdk5 promotes kinesin-mediated transport of membrane bound cargo in squid axoplasm (Ratner *et al*., 1998; Morfini *et al*., 2004).

Because LIN-10 regulates GLR-1 in the VNC and has been implicated in receptor trafficking (Rongo *et al*., 1998; Borg *et al*., 1999; Whitfield *et al*., 1999; Setou *et al*., 2000; Tomita *et al*., 2001; Hill *et al*., 2003; Stricker and Huganir, 2003), we tested whether LIN-10 was required for the effects of CDK-5 on GLR-1. We found that GLR-1::GFP puncta fluorescence intensities in *cdk-5*;*lin-10* double mutants were intermediate in value between those observed in *cdk-5* and *lin-10* single mutants (Figure 9). This result could be interpreted in either of two ways: 1) CDK-5 and LIN-10 function in independent parallel pathways to regulate GLR-1, or 2) CDK-5 regulation of GLR-1 is mediated, in part, through LIN-10, but there are other relevant CDK-5 targets in vivo. We favor the second interpretation for several reasons. Changes in LIN-10 abundance are sufficient to alter GLR-1 in the nerve cord (Figure 6). As detailed above, LIN-10 is likely to be a CDK-5 substrate in vivo, whereby LIN-10 abundance in the nerve cord is negatively regulated by CDK-5. These results strongly support the idea that CDK-5 and LIN-10 are two components of a single biochemical pathway. Nonetheless, further experiments will be required to decisively determine the role of LIN-10 in CDK-5–mediated regulation of GLR-1. Our results do clearly indicate that CDK-5 must have additional targets that contribute to regulating GLR-1. Although we have no direct data bearing on the identity of these targets, two interesting possibilities are the microtubule-associated proteins TAU and MAP1B, both of which are known Cdk5 targets (Pigino *et al*., 1997; Flaherty *et al*., 2000).

CDK-5–mediated regulation of LIN-10/Mint1 abundance provides a potential mechanism coupling CDK-5 activity to the anterograde trafficking process. Several previous studies support the idea that LIN-10/Mint-1 proteins are involved in anterograde transport of GluRs. First, mammalian LIN-10/Mint-1 proteins are localized to the *trans*-Golgi network (TGN), as well as to both pre- and postsynaptic elements (Butz *et al*., 1998; Borg *et al*., 1999; Whitfield *et al*., 1999; Tomita *et al*., 2001; Stricker and Huganir, 2003). Thus, LIN-10/Mint1 proteins are found in subcellular locations consistent with a role in anterograde transport. Second, LIN-10/Mint-1 proteins have been proposed to act as coat proteins that promote budding of cargo into transport vesicles at the TGN (Hill *et al*., 2003). Third, the mouse LIN-10/Mint-1 protein has been proposed to act as a cargo adaptor linking NMDA receptor subunits to the anterograde motor protein KIF17 (Setou *et al*., 2000). Fourth, overexpression of LIN-10/Mint-1 proteins in cultured rat neurons decreases delivery of GluR1 to the cell surface (Stricker and Huganir, 2003).

These studies raise the possibility that LIN-10/Mint-1 and CDK-5 regulate trafficking of GLR-1 from the ER/Golgi to synaptic sites and that they may do so as part of a single biochemical pathway. Our studies also suggest that CDK-5 regulation of GLR-1 is functionally important, because perturbing CDK-5 activity produces changes in GLR-1–mediated behaviors.

Implications for Neurodegeneration and Synaptic Plasticity

Many previous studies have suggested that Cdk5 plays a central role in neurodegeneration. More recent studies have suggested that Cdk5 also regulates synaptic transmission (Fu *et al*., 2001; Fischer *et al*., 2002, 2005; Bibb, 2003; Ohshima *et al*., 2005). Our results provide further support for a potential synaptic function for CDK-5. These results have several potentially interesting implications. It is possible that misregulation of anterograde transport of GluRs contributes to the effects of CDK-5 on neurodegeneration. Increased CDK-5 activity, for example, after cleavage of p35 to the more active p25 by the protease calpain, could predispose neurons to excitotoxicity by increasing the delivery of GluRs to den-

drites and nerve terminals. Conversely, inhibition of CDK-5 activity may provide a useful therapy for mitigating neuron death by potentially decreasing excitotoxicity.

Several studies have suggested that regulated delivery of GluRs to synapses is an important mechanism for expressing activity-dependent synaptic plasticity (Malinow and Malenka, 2002; Song and Huganir, 2002; McGee and Bredt, 2003). In most cases, the activity-dependent step is proposed to be some aspect of endocytic recycling of GluRs at nerve terminals. For example, a recent study shows that delivery of GluRs from recycling endosomes to the synaptic cell surface is the critical step in LTP (Park *et al*., 2004). Other studies suggest that activity also regulates earlier steps in the secretory pathway. For example, chronic activity blockade regulates the splicing of the NMDA receptor subunit NR1 pre-mRNAs, leading to expression of an NR1 isoform that has accelerated exit from the ER (Mu *et al*., 2003). Our studies provide further support for the idea that regulated anterograde transport of GluRs may provide an additional cellular mechanism for synaptic plasticity.

ACKNOWLEDGMENTS

We thank the following for strains, reagents and advice: L. Dreier (UCLA, CA), J. Dittman, J. McEwen (Massachusetts General Hospital, Boston, MA), H. C. Tseng (MIT, MA), L.-H. Tsai, S. Mitani, the *C. elegans* Gene Knockout Consortium, and the *C. elegans* Genetics Center (University of Minnesota, Twin Cities, MN). We thank Emily Malkin for technical assistance and Michele Jacob and members of the Kaplan laboratory for critical comments on this manuscript. This work was supported by grants from the National Institutes of Health (NIH) to J.M.K. (NS32196), and G.G. P.J. was supported by postdoctoral fellowships and NIH grants 1F32NS10957 and NS59953, the American Cancer Society grant PF-00-149-01-CSM, the Massachusetts General Hospital Fund for Medical Discovery, and the March of Dimes (Basil O'Connor Scholar Award).

REFERENCES

Ballif, B. A., Villen, J., Beausoleil, S. A., Schwartz, D., and Gygi, S. P. (2004). Phosphoproteomic analysis of the developing mouse brain. Mol. Cell. Proteomics *3*, 1093–1101.

Berger, A. J., Hart, A. C., and Kaplan, J. M. (1998). G alphas-induced neurodegeneration in *Caenorhabditis elegans*. J. Neurosci. *18*, 2871–2880.

Bibb, J. A. (2003). Role of Cdk5 in neuronal signaling, plasticity, and drug abuse. Neurosignals *12*, 191–199.

Borg, J. P., Lopez-Figueroa, M. O., de Taddeo-Borg, M., Kroon, D. E., Turner, R. S., Watson, S. J., and Margolis, B. (1999). Molecular analysis of the X11-mLin-2/CASK complex in brain. J. Neurosci. *19*, 1307–1316.

Brockie, P. J., Madsen, D. M., Zheng, Y., Mellem, J., and Maricq, A. V. (2001a). Differential expression of glutamate receptor subunits in the nervous system of *Caenorhabditis elegans* and their regulation by the homeodomain protein UNC-42. J. Neurosci. *21*, 1510–1522.

Brockie, P. J., Mellem, J. E., Hills, T., Madsen, D. M., and Maricq, A. V. (2001b). The *C. elegans* glutamate receptor subunit NMR-1 is required for slow NMDA-activated currents that regulate reversal frequency during locomotion. Neuron *31*, 617–630.

Burbea, M., Dreier, L., Dittman, J. S., Grunwald, M. E., and Kaplan, J. M. (2002). Ubiquitin and AP180 regulate the abundance of GLR-1 glutamate receptors at postsynaptic elements in *C. elegans*. Neuron *35*, 107–120.

Butz, S., Okamoto, M., and Sudhof, T. C. (1998). A tripartite protein complex with the potential to couple synaptic vesicle exocytosis to cell adhesion in brain. Cell *94*, 773–782.

Carroll, R. C., Beattie, E. C., Xia, H., Luscher, C., Altschuler, Y., Nicoll, R. A., Malenka, R. C., and von Zastrow, M. (1999). Dynamin-dependent endocytosis of ionotropic glutamate receptors. Proc. Natl. Acad. Sci. USA *96*, 14112–14117.

Colledge, M., Snyder, E. M., Crozier, R. A., Soderling, J. A., Jin, Y., Langeberg, L. K., Lu, H., Bear, M. F., and Scott, J. D. (2003). Ubiquitination regulates PSD-95 degradation and AMPA receptor surface expression. Neuron *40*, 595–607.

Dhavan, R., and Tsai, L. H. (2001). A decade of CDK5. Nat. Rev. Mol. Cell Biol. *2*, 749–759.

Dittman, J. S., and Kaplan, J. M. (2006). Factors regulating the abundance and localization of synaptobrevin in the plasma membrane. Proc. Natl. Acad. Sci. USA *103*, 11399–11404.

Dreier, L., Burbea, M., and Kaplan, J. M. (2005). LIN-23-mediated degradation of beta-catenin regulates the abundance of GLR-1 glutamate receptors in the ventral nerve cord of *C. elegans*. Neuron *46*, 51–64.

Fischer, A., Sananbenesi, F., Pang, P. T., Lu, B., and Tsai, L. H. (2005). Opposing roles of transient and prolonged expression of p25 in synaptic plasticity and hippocampus-dependent memory. Neuron *48*, 825–838.

Fischer, A., Sananbenesi, F., Schrick, C., Spiess, J., and Radulovic, J. (2002). Cyclin-dependent kinase 5 is required for associative learning. J. Neurosci. *22*, 3700–3707.

Flaherty, D. B., Soria, J. P., Tomasiewicz, H. G., and Wood, J. G. (2000). Phosphorylation of human tau protein by microtubule-associated kinases: GSK3beta and cdk5 are key participants. J. Neurosci. Res. *62*, 463–472.

Fletcher, A. I., Shuang, R., Giovannucci, D. R., Zhang, L., Bittner, M. A., and Stuenkel, E. L. (1999). Regulation of exocytosis by cyclin-dependent kinase 5 via phosphorylation of Munc18. J. Biol. Chem. *274*, 4027–4035.

Fu, A. K., Fu, W. Y., Cheung, J., Tsim, K. W., Ip, F. C., Wang, J. H., and Ip, N. Y. (2001). Cdk5 is involved in neuregulin-induced AChR expression at the neuromuscular junction. Nat. Neurosci. *4*, 374–381.

Hart, A. C., Kass, J., Shapiro, J. E., and Kaplan, J. M. (1999). Distinct signaling pathways mediate touch and osmosensory responses in a polymodal sensory neuron. J. Neurosci. *19*, 1952–1958.

Hart, A. C., Sims, S., and Kaplan, J. M. (1995). Synaptic code for sensory modalities revealed by *C. elegans* GLR-1 glutamate receptor. Nature *378*, 82–85.

Hill, K., Li, Y., Bennett, M., McKay, M., Zhu, X., Shern, J., Torre, E., Lah, J. J., Levey, A. I., and Kahn, R. A. (2003). Munc18 interacting proteins: ADP-ribosylation factor-dependent coat proteins that regulate the traffic of β-Alzheimer's precursor protein. J. Biol. Chem. *278*, 36032–36040.

Jorgensen, E. M., Hartwieg, E., Schuske, K., Nonet, M. L., Jin, Y., and Horvitz, H. R. (1995). Defective recycling of synaptic vesicles in synaptotagmin mutants of *Caenorhabditis elegans*. Nature *378*, 196–199.

Juo, P., and Kaplan, J. M. (2004). The anaphase-promoting complex regulates the abundance of GLR-1 glutamate receptors in the ventral nerve cord of *C. elegans*. Curr. Biol. *14*, 2057–2062.

Kaech, S. M., Whitfield, C. W., and Kim, S. K. (1998). The LIN-2/LIN-7/LIN-10 complex mediates basolateral membrane localization of the *C. elegans* EGF receptor LET-23 in vulval epithelial cells. Cell *94*, 761–771.

Kaplan, J. M., and Horvitz, H. R. (1993). A dual mechanosensory and chemosensory neuron in *Caenorhabditis elegans*. Proc. Natl. Acad. Sci. USA *90*, 2227–2231.

Ko, J., Humbert, S., Bronson, R. T., Takahashi, S., Kulkarni, A. B., Li, E., and Tsai, L. H. (2001). p35 and p39 are essential for cyclin-dependent kinase 5 function during neurodevelopment. J. Neurosci. *21*, 6758–6771.

Lee, S. Y., Voronov, S., Letinic, K., Nairn, A. C., Di Paolo, G., and De Camilli, P. (2005). Regulation of the interaction between PIPKI gamma and talin by proline-directed protein kinases. J. Cell Biol. *168*, 789–799.

Lee, S. Y., Wenk, M. R., Kim, Y., Nairn, A. C., and De Camilli, P. (2004). Regulation of synaptojanin 1 by cyclin-dependent kinase 5 at synapses. Proc. Natl. Acad. Sci. USA *101*, 546–551.

Li, B. S., Sun, M. K., Zhang, L., Takahashi, S., Ma, W., Vinade, L., Kulkarni, A. B., Brady, R. O., and Pant, H. C. (2001). Regulation of NMDA receptors by cyclin-dependent kinase-5. Proc. Natl. Acad. Sci. USA *98*, 12742–12747.

Luscher, C., Xia, H., Beattie, E. C., Carroll, R. C., von Zastrow, M., Malenka, R. C., and Nicoll, R. A. (1999). Role of AMPA receptor cycling in synaptic transmission and plasticity. Neuron *24*, 649–658.

Malinow, R., and Malenka, R. C. (2002). AMPA receptor trafficking and synaptic plasticity. Annu. Rev. Neurosci. *25*, 103–126.

Man, H. Y., Lin, J. W., Ju, W. H., Ahmadian, G., Liu, L., Becker, L. E., Sheng, M., and Wang, Y. T. (2000). Regulation of AMPA receptor-mediated synaptic transmission by clathrin-dependent receptor internalization. Neuron *25*, 649–662.

Maricq, A. V., Peckol, E., Driscoll, M., and Bargmann, C. I. (1995). Mechanosensory signalling in *C. elegans* mediated by the GLR-1 glutamate receptor. Nature *378*, 78–81.

McGee, A. W., and Bredt, D. S. (2003). Assembly and plasticity of the glutamatergic postsynaptic specialization. Curr. Opin. Neurobiol. *13*, 111–118.

Morabito, M. A., Sheng, M., and Tsai, L. H. (2004). Cyclin-dependent kinase 5 phosphorylates the N-terminal domain of the postsynaptic density protein PSD-95 in neurons. J. Neurosci. *24*, 865–876.

Morfini, G., Szebenyi, G., Brown, H., Pant, H. C., Pigino, G., DeBoer, S., Beffert, U., and Brady, S. T. (2004). A novel CDK5-dependent pathway for regulating GSK3 activity and kinesin-driven motility in neurons. EMBO J. *23*, 2235–2245.

Mu, Y., Otsuka, T., Horton, A. C., Scott, D. B., and Ehlers, M. D. (2003). Activity-dependent mRNA splicing controls ER export and synaptic delivery of NMDA receptors. Neuron *40*, 581–594.

Nikolic, M., Dudek, H., Kwon, Y. T., Ramos, Y. F., and Tsai, L. H. (1996). The cdk5/p35 kinase is essential for neurite outgrowth during neuronal differentiation. Genes Dev. *10*, 816–825.

Nonet, M. L., Holgado, A. M., Brewer, F., Serpe, C. J., Norbeck, B. A., Holleran, J., Wei, L., Hartwieg, E., Jorgensen, E. M., and Alfonso, A. (1999). UNC-11, a *Caenorhabditis elegans* AP180 homologue, regulates the size and protein composition of synaptic vesicles. Mol. Biol. Cell *10*, 2343–2360.

Ohshima, T. *et al.* (2005). Impairment of hippocampal long-term depression and defective spatial learning and memory in p35 mice. J. Neurochem. *94*, 917–925.

Ohshima, T., Ward, J. M., Huh, C. G., Longenecker, G., Veeranna, Pant, H. C., Brady, R. O., Martin, L. J., and Kulkarni, A. B. (1996). Targeted disruption of the cyclin-dependent kinase 5 gene results in abnormal corticogenesis, neuronal pathology and perinatal death. Proc. Natl. Acad. Sci. USA *93*, 11173–11178.

Park, M., Penick, E. C., Edwards, J. G., Kauer, J. A., and Ehlers, M. D. (2004). Recycling endosomes supply AMPA receptors for LTP. Science *305*, 1972–1975.

Patrick, G. N., Bingol, B., Weld, H. A., and Schuman, E. M. (2003). Ubiquitin-mediated proteasome activity is required for agonist-induced endocytosis of GluRs. Curr. Biol. *13*, 2073–2081.

Pigino, G., Paglini, G., Ulloa, L., Avila, J., and Caceres, A. (1997). Analysis of the expression, distribution and function of cyclin dependent kinase 5 (cdk5) in developing cerebellar macroneurons. J. Cell Sci. *110*, 257–270.

Ratner, N., Bloom, G. S., and Brady, S. T. (1998). A role for cyclin-dependent kinase(s) in the modulation of fast anterograde axonal transport: effects defined by olomoucine and the APC tumor suppressor protein. J. Neurosci. *18*, 7717–7726.

Rongo, C., Whitfield, C. W., Rodal, A., Kim, S. K., and Kaplan, J. M. (1998). LIN-10 is a shared component of the polarized protein localization pathways in neurons and epithelia. Cell *94*, 751–759.

Samuels, B. A., and Tsai, L. H. (2003). Cdk5 is a dynamo at the synapse. Nat. Cell Biol. *5*, 689–690.

Schaefer, H., and Rongo, C. (2006). KEL-8 is a substrate receptor for CUL3-dependent ubiquitin ligase that regulates synaptic glutamate receptor turnover. Mol. Biol. Cell *17*, 1250–1260.

Schuske, K. R., Richmond, J. E., Matthies, D. S., Davis, W. S., Runz, S., Rube, D. A., van der Bliek, A. M., and Jorgensen, E. M. (2003). Endophilin is required for synaptic vesicle endocytosis by localizing synaptojanin. Neuron *40*, 749–762.

Setou, M., Nakagawa, T., Seog, D. H., and Hirokawa, N. (2000). Kinesin superfamily motor protein KIF17 and mLin-10 in NMDA receptor-containing vesicle transport. Science *288*, 1796–1802.

Song, I., and Huganir, R. L. (2002). Regulation of AMPA receptors during synaptic plasticity. Trends Neurosci. *25*, 578–588.

Stricker, N. L., and Huganir, R. L. (2003). The PDZ domains of mLin-10 regulate its trans-Golgi network targeting and the surface expression of AMPA receptors. Neuropharmacology *45*, 837–848.

Tomita, S., Nicoll, R. A., and Bredt, D. S. (2001). PDZ protein interactions regulating glutamate receptor function and plasticity. J. Cell Biol. *153*, F19–F24.

Tomizawa, K., Ohta, J., Matsushita, M., Moriwaki, A., Li, S. T., Takei, K., and Matsui, H. (2002). Cdk5/p35 regulates neurotransmitter release through phosphorylation and downregulation of P/Q-type voltage-dependent calcium channel activity. J. Neurosci. *22*, 2590–2597.

Wang, J., Liu, S., Fu, Y., Wang, J. H., and Lu, Y. (2003). Cdk5 activation induces hippocampal CA1 cell death by directly phosphorylating NMDA receptors. Nat. Neurosci. *6*, 1039–1047.

Whitfield, C. W., Benard, C., Barnes, T., Hekimi, S., and Kim, S. K. (1999). Basolateral localization of the *Caenorhabditis elegans* epidermal growth factor receptor in epithelial cells by the PDZ protein LIN-10. Mol. Biol. Cell *10*, 2087–2100.

Zhang, B., Koh, Y. H., Beckstead, R. B., Budnik, V., Ganetzky, B., and Bellen, H. J. (1998). Synaptic vesicle size and number are regulated by a clathrin adaptor protein required for endocytosis. Neuron *21*, 1465–1475.

Zheng, Y., Brockie, P. J., Mellem, J. E., Madsen, D. M., and Maricq, A. V. (1999). Neuronal control of locomotion in *C. elegans* is modified by a dominant mutation in the GLR-1 ionotropic glutamate receptor. Neuron *24*, 347–361.